Analytical energy-barrier-dependent V_{oc} model for amorphous silicon solar cells

A. Castro-Carranza,[1,a)] J. C. Nolasco,[2,a)] N. Reininghaus,[3] S. Geißendörfer,[3] M. Vehse,[3] J. Parisi,[2] J. Gutowski,[1,4] and T. Voss[5,6]
[1]*Institute of Solid State Physics, University of Bremen, 28359 Bremen, Germany*
[2]*Energy and Semiconductor Research Laboratory, Carl von Ossietzky University of Oldenburg, 26129 Oldenburg, Germany*
[3]*NEXT ENERGY-EWE Research Centre for Energy Technology at Carl von Ossietzky University of Oldenburg, 26129 Oldenburg, Germany*
[4]*MAPEX Center of Materials and Processes, University of Bremen, 28359 Bremen, Germany*
[5]*Institute of Semiconductor Technology, Braunschweig University of Technology, 38092 Braunschweig, Germany*
[6]*Laboratory for Emerging Nanometrology (LENA), Braunschweig University of Technology, 38092 Braunschweig, Germany*

(Received 18 April 2016; accepted 14 July 2016; published online 27 July 2016)

We show that the open circuit voltage (V_{oc}) in hydrogenated amorphous silicon (a-Si:H) solar cells can be described by an analytical energy-barrier-dependent equation, considering thermionic emission as the physical mechanism determining the recombination current. For this purpose, the current-voltage characteristics of two device structures, i.e., a-Si:H(n)/a-Si:H(i)/a-Si:H(p)/AZO p-i-n solar cells with different p-doping concentrations and a-Si:H(n)/a-Si:H(i)/AZO Schottky structures with different intrinsic layer thicknesses, were analyzed in dark and under illumination, respectively. The calculated barrier in the p-i-n devices is consistent with the difference between the work function of the p-layer and the conduction band edge of the i-layer at the interface in thermal equilibrium. *Published by AIP Publishing.* [http://dx.doi.org/10.1063/1.4959939]

The open circuit voltage (V_{oc}) is one of the fundamental parameters defining the efficiency (η) of solar cells. It is fundamentally determined by the difference of hole and electron quasi-Fermi levels of an illuminated cell with open contacts and, hence, at zero external current. The difference between the quasi-Fermi levels can be to a large extent directly related to the bulk properties of the active materials or to the interfaces within the cells. In p-i-n solar cells based on amorphous silicon, extensive experimental work showed the impact of different technological factors on the device performance. For example, V_{oc} changes were obtained by modifying the bulk properties of the intrinsic absorber layer, such as its band gap[1] or doping,[2] and by light soaking.[3] Furthermore, by modifying the interface properties through, e.g., variation of the p and n layers,[4,5] introduction of buffer layers,[5] and by use of different transparent conductive oxide (TCO) materials.[6] All these experimental evidences indicate that both the bulk and the interfaces substantially affect V_{oc}. Assuming optimized interfaces, the phenomena in the bulk have been described by the drift-diffusion model considering band-to-band recombination. More elaborated models considered recombination through trap states.[7] Other studies suggested that V_{oc} is ultimately determined by interfacial properties. For example, by using numerical simulations, Jiang *et al.* showed that thermionic emission of carriers over an interfacial barrier at the p side being caused by a band discontinuity could be the foundation of a V_{oc} model based on interface physics.[8] A related effect of the back contact on V_{oc}, known as "back surface field," was documented earlier by Mandelkorn and Lamneck for p+/p crystalline silicon junctions.[9] This effect has been one of the milestones to increase the V_{oc} values in such cells.[10] The impact of the contacts on V_{oc} has been typically quantified by considering an effective interface recombination velocity.[11] However, when using such an approach, the reduction of the surface field by an applied potential that affects the recombination velocity results in a non-trivial analytical relation.[12] Here, we show that a simpler and consistent approach to quantify the effect of such interfacial phenomena on V_{oc} in p-i-n a-Si:H solar cells is obtained by considering a thermionic emission mechanism in the interface with the lowest potential barrier. This mechanism cannot be described by a barrier resulting from a band discontinuity at the p-i interface but by a barrier given by the difference between the work function of the p-type semiconductor and the conduction band edge of the intrinsic material, which is consistent with both our experimental observation and band-diagram simulations.

The model is validated for two kinds of solar cell structures: a-Si:H(n)/a-Si:H(i)/a-Si:H(p)/AZO p-i-n solar cells with four different p-doping concentrations, and a-Si:H(n)/a-Si:H(i)/AZO Schottky structures with three different i-layer thicknesses. For this purpose, we first focus on the modeling of the dark characteristics to analyze the saturation current J_0 using an equivalent circuit. Then, the corresponding barrier height is calculated with the thermionic-emission current model and used in the proposed model to calculate V_{oc}. The so-obtained values were compared to the experimentally extracted V_{oc} values under illumination. Finally, band-diagram simulations are performed to validate our

[a)]Authors to whom correspondence should be addressed. Electronic addresses: a.castroc@ifp.uni-bremen.de and jairo.cesar.nolasco.montano@uni-oldenburg.de

calculated values of the barrier height based on the thermionic emission theory.

The a-Si:H solar cell structures are deposited in p-i-n sequence (p-doped with B_2H_6 (20 nm)/intrinsic (450 nm)/n-doped with PH_3 (20 nm)) using a plasma enhanced chemical vapor deposition (PECVD) reactor from Leybold Optics under a pressure of 4 mbar and a substrate temperature between 190° and 220°. The solar cells are deposited using a 13.56 MHz plasma excitation frequency at narrow electrode gap (10 mm). $10 \times 10\,cm^2$ ZnO:Al coated glass (with 2% Al content) serves as a substrate for the single junction cells. 300 nm thick Ag back contact pads prepared by electron beam evaporation define the cell areas of $1\,cm^2$. After deposition, all solar cells are annealed for 30 min at 160 °C. All samples were deposited with the same procedure except for the B_2H_6 flow during the p-layer deposition which was varied from 0 to 8.8 sccm in steps of 1.7 sccm. In the case of the a-Si:H(n)/a-Si:H(i)/AZO Schottky solar cell configuration, intrinsic a-Si:H layers of different thickness, i.e., $i_a = 100$, $i_b = 200$, and $i_c = 300$ nm, were deposited on AZO substrates, followed by an n-doped a-Si:H layer of 25 nm thickness. The areas of these cells are $0.8\,cm^2$. The respective schematic structures are shown in Fig. 1, indicating the interface under study where the lowest potential barrier is expected.

Current density vs. voltage (J–V) characteristics of the devices were measured at room temperature in dark and under illumination (AM 1.5 g, $1000\,W/cm^2$, 25 °C) using a continuous light (DC) sun simulator of class A (WACOM WXS-155S-L2-AM1.5GMM) and an Autolab PGSTAT302N. Fig. 2 shows the experimental characteristics of the a-Si:H p-i-n solar cells with different p-doping under illumination (filled symbols) and in dark (empty symbols). Similarly, Fig. 3 shows the characteristics of the Schottky devices and compared with the p-i-n device with the highest efficiency, i.e., with 3.4 sccm B_2H_6 used. The J–V characteristics at relative intermediate voltage values of both types of devices are similar concerning the slope of the linear section. The Schottky solar cell with an intrinsic layer thickness of 300 nm differs from the other cells in the low-voltage region, indicating a larger leakage current density within the junction. Among the characteristics, the 0 sccm sample presents particular differences, mainly at high voltages, due to the relative increment of its intrinsic layer thickness. The linear section is determined by the diode formed in the structure. Its slope corresponds to the ideality factor m of the diode, and the intersection of the line with the current density axis corresponds to J_0.

The voltage dependent current density J in dark is modeled using the circuit depicted in the inset of Fig. 2 by fitting the well known general equation[13]

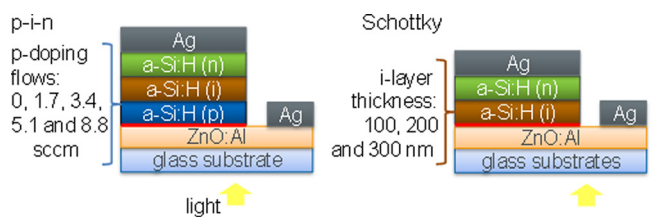

FIG. 1. Schematic structures of both the a-Si:H p-i-n solar cell (left) fabricated with different p-doping flows, and the Si:H(i)/a-Si:H(n) Schottky solar cells (right), with different i-layer thicknesses. The interfaces under study to which losses are mainly attributed are indicated with a red line, respectively.

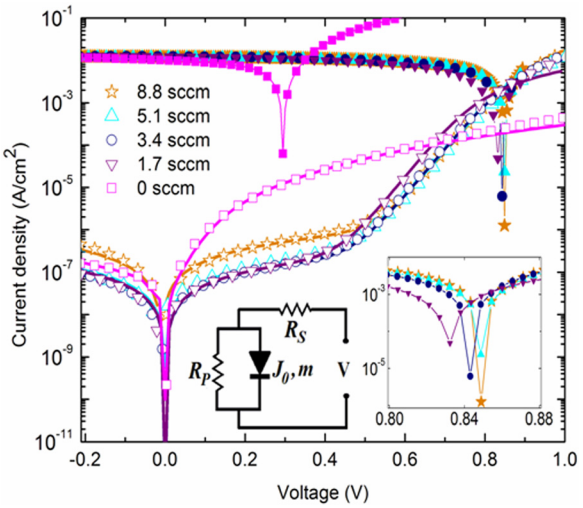

FIG. 2. Experimental (symbols) and modeled (thick lines) J–V characteristics of a-Si:H p-i-n solar cells for different p-doping flows under dark (empty symbols) and under illumination (filled symbols) conditions. Inset: Circuit model (left) and a zoom-in of the characteristics under illumination showing the experimental V_{OC} values (right).

$$J = J_0\left[\exp\left[\frac{q(V - JAR_s)}{mk_BT}\right] - 1\right] + \frac{V - JAR_s}{R_pA}, \qquad (1)$$

where V is the applied bias, k_B the Boltzmann constant, T the temperature, and A the active area of the device. R_P is the parallel resistance describing the leakage of the junction at low voltage values. R_S is the series resistance attributed to the bulk whose effect is given in the range from medium to high voltage, following the linear region defined by the diode in the J–V characteristics. The extracted parameters in dark are listed in Table I together with the photovoltaic parameters calculated from the measurement setup under illumination, i.e., the short circuit current density J_{sc}, the experimental value of V_{oc}, the fill factor FF, and the device efficiency η. The reproducibility of the experiment has been verified. The p-doped

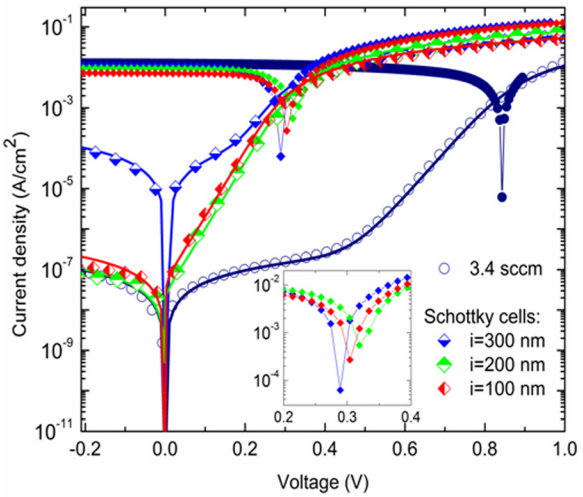

FIG. 3. Experimental (symbols) and modeled (lines) J–V characteristics of AZO/a-Si:H(i)/a-Si:H(n) Schottky solar cells (diamonds) for different intrinsic layer thicknesses compared with the p-i-n solar cell fabricated using 3.4 sccm B_2H_6 (circles) under dark (empty symbols) and under illumination (filled symbols) conditions. Inset: zoom-in of the characteristics under illumination showing the experimental V_{OC} values.

TABLE I. Parameters extracted under dark and illumination conditions.

	Illumination				Dark			
Device	J_{SC} (mA/cm^2)	V_{OC} (mV)	FF (%)	η (%)	J_0 (mA/cm^2)	m	Rs (Ω/cm^2)	Rp (Ω/cm^2)
p-i-n								
8.8 sccm	12.19	850	50	5.16	1.0×10^{-9}	1.55	7	2.4×10^6
5.1 sccm	12.15	848	49	5.10	1.1×10^{-9}	1.55	10	1.8×10^6
3.4 sccm	12.51	843	53	5.62	1.2×10^{-9}	1.50	10	2.1×10^6
1.7 sccm	12.22	832	46	4.57	2.0×10^{-9}	1.45	32	2.0×10^6
0 sccm	12.58	306	36	1.38	3.0×10^{-5}	1	2×10^4	1.2×10^6
Schottky								
$i_a = 100$ nm	7.06	306.92	57.15	1.24	4.0×10^{-5}	1	12	1.0×10^6
$i_b = 200$ nm	9.24	324.12	54.65	1.64	2.0×10^{-5}	1	8	2.0×10^6
$i_c = 30\,0$ nm	10.42	288.12	49.43	1.49	1.0×10^{-4}	1	10	2.0×10^3

samples present certain variation; thus, we used an average of 15 devices for each structure. The qualitative behavior of V_{oc} agrees with that observed in a-Si:H solar cells in the literature, i.e., V_{oc} decreases for increasing intrinsic layer thickness,[13] and it increases for higher p-doping levels in a-Si:H heterojunction wafer based solar cells.[5]

The extracted ideality factors m, equal and close to unity in the case of the Schottky and p-i-n solar cells, respectively, indicate that the J–V characteristics of the devices under dark condition can be described by either considerations of drift-diffusion currents or thermionic emission.[14,15] Both mechanisms rely on the existence of an internal electrostatic field, and since these mechanisms occur in series, the current in the devices will be determined by the contribution with the largest impediment to the flow of charge. The drift-diffusion model more accurately describes the electrical behavior in case that recombination in the depletion region is significant,[14] whereas thermionic emission holds when the carriers lose their potential energy at the interface barrier.[16] Thermionic emission is the most fundamental conduction mechanism occurring in metal/semiconductor or semiconductor interface junctions.[15] In this mechanism, the portion of the thermally generated carriers increases as the internal built-in electric field decreases with the applied potential at the respective junction, so they contribute to the thermionic-emission current by overcoming the interfacial barrier with height ϕ_b. J_0 is the component of the voltage dependent current density that remains unaffected by the applied potential, which accounts for the charge carrier recombination losses in a solar cell. According to thermionic emission theory, it is given by

$$J_0 = A^* T^2 \exp(-q\phi_b / k_B T), \tag{2}$$

where A^* is the effective Richardson coefficient for free carriers taken as $A^* = 120$ A/cm^2 K^2.[14]

An analytical barrier-dependent V_{oc} model is obtained by introducing Eq. (2) in the well-known V_{oc} expression

$$V_{oc} = \frac{mk_B T}{q \ln(J_{sc}/J_0)}, \tag{3}$$

which is, in turn, obtained by considering open-circuit conditions ($J = 0$) and assuming the last term in Eq. (1) to be negligible due to high R_p values.[17] The obtained barrier-dependent V_{oc} model is

$$V_{oc} = m\phi_b - \frac{mk_B T}{q} \ln\left(\frac{A^* T^2}{J_{sc}}\right). \tag{4}$$

This expression is expected to accurately describe V_{oc} when $1 < m < 2$.[18] In the second term of Eq. (4), the linear temperature dependence is dominant over the logarithmic one. This means that the linear dependence of V_{oc} on temperature in a-Si:H solar cells[19] is well predicted by Eq. (3) which also describes the well-known linear relation between V_{oc} and the logarithm of J_{sc} which in turn depends on the light intensity.[8] These characteristics are typical not only for a-Si:H solar cells but also for devices based on other thin film technologies such as organics and CIGS semiconductors.[17,20] To verify the latter analytical barrier-dependent model, we calculate V_{oc} for the studied cells by using the extracted J_0, the ideality factor, and the barrier height obtained from Eq. (2). The calculated values for ϕ_b and V_{oc} are listed in Table II for both solar cell structures.

Good agreement is obtained when comparing V_{oc} experimentally determined from the measurement under illumination (Table I) and V_{oc} calculated with Eq. (4) (Table II). Hence, a clear correlation of ϕ_b with V_{oc} is obvious for the two different structures. The latter confirms that the obtained V_{oc} values can be well described by thermionic emission.

TABLE II. Comparison of barrier heights ϕ_b as calculated with Eq. (2) and open-circuit voltage V_{oc} as calculated with Eq. (4) for the p-i-n and the three Schottky solar cells with different intrinsic layer thicknesses.

Device	ϕ_b (meV)	V_{OC} (mV)
p-i-n		
8.8 sccm	1133	915
5.1 sccm	1131	909
3.4 sccm	1128	895
1.7 sccm	1115	845
0 sccm	877	345
Schottky		
$i_a = 100$ nm	863	313
$i_b = 200$ nm	881	338
$i_c = 300$ nm	840	300

To validate the calculated barrier height, band-diagram simulations for both kinds of cells were performed in AFORS-HET,[21] using the default parameters of a standard p-i-n solar cell, Table SI (supplementary material).[22] The band-diagram simulations for a p-i-n solar cell and the Schottky device with $i_c = 300$ nm are shown in Figs. 4(a) and 4(b), respectively. According to thermionic emission theory, ϕ_b in Schottky junctions is given by the difference between the work function of the metal (Φ_m) and the valence or conduction band edge of the p- or n-type semiconductor, respectively. In a semiconductor/semiconductor junction, ϕ_b corresponds to the difference between the work function of the semiconductor with the highest carrier concentration and the corresponding majority carrier band edge of the semiconductor with a lower concentration. Thus, assuming that the dominant recombination occurs on the p side, the barrier formed in the p-i-n solar cell is given by $\phi_{bp} = \Phi_{(p)} - E_{C(i)}$ while in the Schottky devices, we have $\phi_{b_{AZO}} = \Phi_m - E_{C(i)}$, where $\Phi_{(p)}$ is the work function of the p-type semiconductor, $E_{C(i)}$ the conduction band edge of the intrinsic material, and Φ_m corresponds to the work function of the AZO. The barrier heights for the respective kind of simulated device are 1.27 eV and 0.75 eV, as indicated in Fig. 4.

According to the simulated band diagrams of the p-i-n solar cell and the Schottky devices in Figs. 4(a) and 4(b), respectively, we found a clear correspondence between the barriers ϕ_b calculated using Eq. (4) based on thermionic emission theory (Table II) and ϕ_{bp} obtained for p-i-n solar cells and $\phi_{b_{AZO}}$ for Schottky devices. The barrier at the n side is higher than that at the p side and the TCO in the respective structures. Thus, our result indicates that charge recombination occurs on the side with the barrier of lowest height (see Fig. 4). Our finding also demonstrates that the thermionic emission mechanism can describe V_{oc} in agreement with the results of Schiff *et al.*,[7,8] but by accounting for an energy-barrier defined by the difference of the Fermi level of the p-type semiconductor and the conduction band edge of the intrinsic material at the heterojunction, and not by accounting for a discontinuity in the conduction band as suggested in the studies cited. Since the built-in potential (V_{bi}) depends on the work function of the p-type material in p-i-n solar cells, a variation of the height of ϕ_b could affect the charge transport along the intrinsic layer.

Note that Eq. (1) is a non-ideal general diode expression and that the ideal Shockley model corresponds to the specific case when $m = 1$ and J_0 is determined by band-to-band recombination of the minority carriers.[14] For the case of ideal thermionic emission, m holds 1, and J_0 is determined by the generation-recombination of majority carriers at ϕ_b. Our results show that J_0 is determined by ϕ_b. This conclusion is drawn based on three outcomes. First, the calculated values of ϕ_b vary with the Fermi level defined by the p-doping. Second, ϕ_b depends on the interface modification as done for the Schottky devices. Finally, a consistent estimation of V_{oc} is obtained using ϕ_b. In addition, following the same procedure as described above, we calculated V_{oc} for a-Si:H/c-Si heterojunction solar cells using Eq. (4) and the reported values in literature[23] at 300 K ($m = 1.05$, $J_{sc} = 26.65$ mA/cm^2, and $J_0 = 5.05 \times 10^{-9}$ mA/cm^2) yielding 609 mV. This value is comparable to the experimental result of 650 mV. A second procedure is to calculate V_{oc} using the activation energy (E_a) from a modified Arrhenius plot obtained from J_0-temperature characteristics. The calculation consists of considering ϕ_b as E_a (1.14 eV (Ref. 23)) in Eq. (4). This yields 660 mV which is consistent to the experimental result.

The deviation of m from one as the barrier increases is a sign of this phenomenon, since $m > 1$ values are usually attributed to a contribution of voltage dependent recombination mechanisms as the one assisted by tunneling.[15,24] The increase of m in the p-i-n samples with a higher p doping concentration is hence attributed to additional charge recombination assisted by tunneling through ϕ_b. This yields an increase of error in the prediction of V_{oc} for devices with relatively high m as can be seen in Table I. On this basis, our proposed barrier model allows to unify the effects of both the doping of the p-type layer (corresponding to the lowest barrier) and the recombination losses occurring in the intrinsic layer on V_{oc}, which have been considered separately as two different models for p-i-n cells.[25]

The observed constant value of m even for different i-layer thicknesses in the Schottky solar cells confirms that J_0 is determined by charge recombination occurring at the i-layer/TCO interface which is consistent with a thermionic emission mechanism. According to Eq. (4), the barrier is sensitive to both the conduction band edge of the intrinsic material and the Fermi level of the material with highest carrier concentration. The observed variation of the barrier height with the thickness of the intrinsic layer (see Table II) indicates that bulk modifications just slightly affect the effective

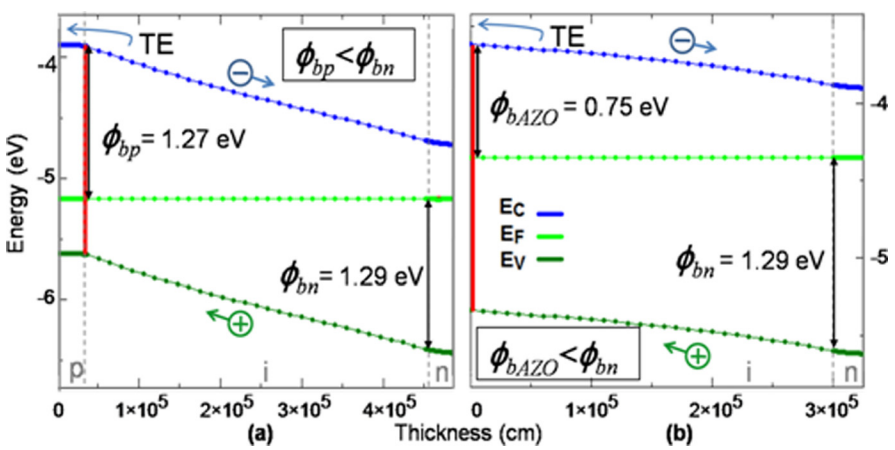

FIG. 4. Band diagram simulated in AFORS-HET of the (a) standard p-i-n a-Si:H/AZO solar cell, (b) a-(n)Si:H/(i)Si:H/AZO Schottky solar cell with $i_c = 300$ nm. The interfaces under study to which losses are mainly attributed are indicated with a red line, respectively. TE is the thermionic emission, E_C is the conduction band edge, E_F is the Fermi level, and E_V is the valence band edge.

barrier (~5%). Small impact on V_{oc} has been usually observed in p-i-n solar cells with different intrinsic layer thicknesses.[13] It should be mentioned that an additional barrier can be formed between the p-type material and the TCO which can affect the extraction of holes.[26–28] The prediction of V_{oc} by Eq. (4) indicates that such a phenomenon does not occur in the cells studied here.

Given that the ideality factors of the studied devices approach one, it is considered to have low defect state densities at the junction.[29] The values of V_{oc}, the low FF, and J_{sc} are comparable to record efficiency devices ($V_{oc} = 0.89$ V, FF = 75, and $J_{sc} = 16.10\,\text{mA/cm}^2$).[30] Therefore, the low efficiency of the studied devices is attributed to charge collection losses in the bulk.

In conclusion, by analyzing the current-voltage characteristics of a-Si:H(n)/a-Si:H(i)/a-Si:H(p)/AZO p-i-n solar cells with different p-type doping flows and a-Si:H(n)/a-Si:H(i)/AZO Schottky devices with different intrinsic layer thicknesses, we have demonstrated that their V_{oc} can be predicted by a thermionic emission model (see Eq. (4)). Furthermore, the energy barriers ϕ_b calculated by this analytical barrier-dependent V_{oc} model are consistent with the difference of the work function of the material with a higher charge concentration and the conduction band edge of the intrinsic material at the interface in a band diagram at thermal equilibrium for both kinds of structures, in agreement with thermionic emission theory. These results, the consistence of our proposed energy-barrier-dependent V_{oc} model that we earlier developed for organic solar cells[18] and the fundamental generality of the thermionic emission mechanism, indicate that such a model can be applied to other thin film solar cell technologies to predict V_{oc}.

A.C.-C. was supported by the combined University of Bremen/FP7-PEOPLE-2012 COFUND Marie-Curie Fellowship "BREMEN TRAC," Project No. 600411. J.C. Nolasco acknowledges the Alexander von Humboldt Foundation for the Georg Foster postdoctoral grant.

[1]J. M. Pearce, N. Podraza, R. W. Collins, M. M. Al-Jassim, K. M. Jones, J. Deng, and C. R. Wronski, J. Appl. Phys. **101**, 114301 (2007).
[2]M. Hack and M. S. Shur, J. Appl. Phys. **55**, 4413 (1984).
[3]M. Isomura, M. Kondo, and A. Matsuda, Jpn. J. Appl. Phys. **39**, 3339 (2000).
[4]G. Bugnon, G. Parascandolo, S. Hänni, M. Stuckelberger, M. Charrière, D. Matthieu, F. Sculati-Meillaud, and C. Ballif, Sol. Energy Mater. Sol. Cells **120**, 143 (2014).
[5]O. M. Ghahfarokhi, K. von Maydell, and C. Agert, Appl. Phys. Lett. **104**, 113901 (2014).
[6]F-J. Haug, R. Biron, G. Kratzer, F. Leresche, J. Besuchet, C. Ballif, M. Dissel, S. Kretschmer, W. Soppe, P. Lippens, and K. Leitner, Prog. Photovoltaic: Res. Appl. **20**, 727 (2012).
[7]E. A. Schiff, Sol. Energy Mater. Sol. Cells **78**, 567 (2003).
[8]L. Jiang, J. H. Lyou, S. Rane, E. A. Schiff, Q. Wang, and Q. Yuan, MRS Proc. **609**, A1831–A18311 (2000).
[9]J. Mandelkorn and J. H. Lamneck, Jr., J. Appl. Phys. **44**, 4785 (1973).
[10]M. A. Green, *Silicon Solar Cells: Advanced Principles and Practice, Centre for Photovoltaics Devices and Systems* (N.S.W, Kensington, 1995).
[11]N. Jensen, U. Rau, R. M. Hausner, S. Uppal, L. Oberbeck, R. B. Bergmann, and J. H. Werner, J. Appl. Phys. **87**, 2639 (2000).
[12]K. Taretto, Prog. Photovoltaic: Res. Appl. **22**, 870 (2014).
[13]A. Luque and S. Hegedus, *Handbook of Photovoltaic Science and Engineering*, 2nd ed. (Wiley, Hoboken, NJ, 2011).
[14]S. M. Sze, *Physics of Semiconductor Devices*, 3rd ed. (John Wiley-Interscience, New York, 1979).
[15]A. G. Milnes and D. L. Feucht, *Heterojunctions and Metal-Semiconductor Junctions* (Academic Press, New York, 1972).
[16]E. H. Rhoderick and R. H. Williams, *Metal-Semiconductor Contacts*, 2nd ed. (Oxford University Press, New York, 1988).
[17]A. McEvoy, T. Markvart, and L. Castañer, *Practical Handbook of Photovoltaics Fundamental and Applications*, 2nd ed. (Elsevier, USA, 2011).
[18]J. C. Nolasco, G. Ramos-Ortiz, J. L. Maldonado, O. Barbosa-Garcia, B. Ecker, and E. von Hauff, Appl. Phys. Lett. **104**, 043308 (2014).
[19]J. Liang, E. A. Schiff, S. Guha, B. Yan, and J. Yang, Appl. Phys. Lett. **88**, 063512 (2006).
[20]J. Widmer, M. Tietze, K. Leo, and M. Riede, Adv. Funct. Mater. **23**, 5814–5821 (2013).
[21]M. Schmidt, L. Korte, A. Laades, R. Stangl, C. Schubert, H. Angermann, E. Conrad, and K. v. Maydell, Thin Solid Films **515**, 7475 (2007).
[22]See supplementary material at http://dx.doi.org/10.1063/1.4959939 for the default simulation parameters used in AFORS-HET for a-Si:H pin solar cells.
[23]N. Jensen, R. M. Hausner, R. B. Bergmann, J. H. Werner, and U. Rau, Prog. Photovoltaic: Res. Appl. **10**, 1–13 (2002).
[24]J. M. Pearce, R. J. Koval, A. S. Ferlauto, R. W. Collins, C. R. Wronski, J. Yang, and S. Guha, Appl. Phys. Lett. **77**, 3093 (2000).
[25]R. Biron, C. Pahud, F. Haug, and C. Ballif, J. Non-Cryst. Solids **358**, 1958 (2012).
[26]A. N. Corpus-Mendoza, M. M. de Souza, and F. Hamelmann, J. Appl. Phys. **114**, 184505 (2013).
[27]M. Bivour, C. Reichel, M. Hermle, and S. W. Glunz, Sol. Energy Mater. Solar Cells **106**, 11 (2012).
[28]F. A. Rubinelli, J. K. Arch, and S. J. Fonash, J. Appl. Phys. **72**, 1621 (1992).
[29]R. T. Tung, Appl. Phys. Rev. **1**, 011304 (2014).
[30]T. Matsui, A. Bidiville, K. Maejima, H. Sai, T. Koida, T. Suezaki, M. Matsumoto, K. Saito, I. Yoshida, and M. Kondo, Appl. Phys. Lett. **106**, 053901 (2015).